DEPENDENCE OF RMP PENETRATION THRESHOLD ON PLASMA PARAMETERS AND ION SPECIES IN HELICAL PLASMAS

K.Y. WATANABE[1,2], S. SAKAKIBARA[1,3], Y. NARUSHIMA[1,3], S. OHDACHI[1,4], Y. SUZUKI[1,3], Y. TAKEMURA[1,3], K. IDA[1,3], M. YOSHINUMA[1,3], I. YAMADA[1] and LHD EXPERIMENT GROUP

[1]National Institute for Fusion Science, National Institutes of Natural Science, Toki, Gifu 509-5292,Japan
[2]Nagoya University, Graduate School of Engineering, Chikusa, Nagoya, 464-8603, Japan
[3]SOKENDAI (The Graduate University for Advanced Studies), Toki, Gifu 509-5292, Japan
[4]The University of Tokyo, Graduate School of Frontier Sciences, Kashiwa, Chiba 277-8561, Japan

Abstract

We investigate the penetration threshold of the RMP (Resonant Magnetic Perturbation) by the external coils in the LHD (Large Helical Device) for the various plasma aspect ratio configurations. The qualitative dependence on the collisionality is opposite to that in a high plasma aspect configuration, which is a quite unique property, and it is first found in the LHD. We also investigate the threshold dependence on the ion species, and find that the threshold in the deuterium discharges is quite smaller than that in the hydrogen discharges. In all of the cases, the thresholds are higher as the poloidal rotation is faster, which shows that the poloidal rotation is the dominant driver to the RMP threshold. It is qualitatively consistent with the torque balance model between the electro-magnetic and the poloidal viscous torque. In a configuration of the LHD, the threshold dependence on the density is qualitatively similar with that in Ohmic tokamak plasmas, but the beta dependence is opposite to that of the tokamaks. The difference would come from the cause of the viscous torque.

1. INTRODUCTION

Existence of the intrinsic RMP (Resonant Magnetic Perturbation), which is the same with "error field", induces the magnetic island and leads to the degradation of plasma confinement in helical plasmas. In tokamaks, the RMP induces the locked-mode instability, which sometimes leads to a disruption. At other times, the RMP becomes a "seed island" on the neoclassical tearing instability, which limits the operational beta value. On the other hand, the RMP is applied as the effective control knob to improve the confinement performance in the torus plasmas. For example, in tokamaks, the RMP is applied to control the RWM (Resistive Wall Mode) [1] and the ELM [2].

However, even if the RMP is externally imposed, the island does not always appear in plasmas. In the LHD [3], which is one of the largest helical devices in the world, the island sometimes appears and in the other times does not appear in the plasma region depending on the plasma parameters while the external RMP is imposed [4, 5]. In the LHD, it is also reported that there is a threshold of the RMP penetration, which means that the island is not observed when the amplitude of the external RMP does not exceed a value (threshold), but it appears when the amplitude is beyond the value [6, 7]. In tokamaks, the locked mode instability does not always appear when the tearing instability is expected to be unstable and the external RMP (error field) exists. The locked mode instability is often observed when the amplitude of the RMP is beyond a value (threshold), too [8]. The above phenomena are observed under the condition that the external RMP does not rotate in time. Even in the case that the RMP rotates, it is also reported that the RMP is shielded or decreases in the plasma when the amplitude is below a value, and the RMP is amplified when the amplitude is beyond the value [9].

In particular, in ITER, the tolerance of the error field to avoid the locked mode instability is an important concern because the locked mode and the disruption as the post process are expected in Ohmic discharges. Here the minimum amplitude of the RMP to induce the locked mode instability is considered as the threshold of the RMP penetration. The construction of an empirical scaling on RMP penetration threshold has been attempted based on the experiments in the multi-devices for many years [8, 10]. On the other hand, the theoretical models of the RMP shielding mechanism by the plasmas and the determination of the RMP penetration threshold are investigated [11, 12]. However, the empirical scaling of the RMP penetration threshold and the theoretical model on the determination of the threshold should be investigated to further improve the prediction accuracy.

In the LHD, the RMP is applied as a control knob to improve the confinement performance. For example, the RMP is applied to maintain a "stable" detached discharge [13], to control the ELM [14], and to control the resistive interchange MHD instability [15]. Figure 1 shows the magnetic fluctuation amplitude (a) and the phase

(defined by the poloidal location of the island's O-point at a toroidal cross-section) of m/n=1/1 RMP component induced by plasma as the function of the imposed RMP coil current. The fluctuation amplitude decreases as the imposed RMP coil current increases. It should be noticed that the phase of m/n=1/1 RMP component induced by plasma does not change until $I_{RMP\text{-}p}/B_t$~1.14kA/T, which corresponds to a boundary between the RMP is shielded and it partially penetrates. This result suggests that the MHD instability is suppressed just before the RMP penetrates plasmas. Then, in the helical systems, it is important to construct the empirical scaling and understand the determination model of the RMP penetration threshold, too.

In the LHD, the RMP shielding mechanism and the determination model of the penetration threshold have been intensively investigated [4-7, 16, 17, 18] since the RMP shielding phenomena were newly observed in the LHD [19]. In Ref.[5], the healing and growing (shielding and penetration) conditions of the external RMP are summarized in the beta value and collisionality spaces, and the bootstrap current modified by the island was considered as the shielding effect. But, the effect of the bootstrap current does not explain the experimental results. In Ref.[16], the observation of the time evolution of the poloidal flow at the transition phase of the island healing/growing suggests that the evolution of the poloidal flow at the outside of the resonant rational surface is strongly related with the RMP shielding threshold. In Refs.[7, 17], the dependence of the RMP penetration/shielding threshold on the magnetic configurations is reported. The plasma aspect ratio dependence of the penetration threshold is strongly related with the index of the interchange MHD instability such as the Mercier parameter, D_I, because the threshold increases with the decrease of the magnetic shear and the increase of the magnetic hill parameter. On the contrary, the magnetic axis location dependence is consistently explained by the effect of the neoclassical viscos torque. Then, we could not explain the reason why the magnetic configuration dependence of the RMP penetration threshold appears.

This paper is organized as follows. First, we show the experiment setup, the wave forms of a typical RMP ramp-up experiments, and some configuration features of the LHD in section 2. The typical experimental conditions are also shown. The RMP penetration threshold dependence on the collisionality for the various plasma aspect ratio configurations are compared in order to improve the database of the penetration threshold dependence on the magnetic configurations, which are shown in section 3.1. In section 3.2, the RMP penetration threshold in the recent deuterium experiments is investigated, and the threshold is compared with that in the hydrogen plasmas from the viewpoint of the ion species dependence of the RMP penetration threshold. In section 3.3, we discuss the above results from the viewpoint of the relationship between the RMP penetration threshold and the plasma poloidal velocity. In section 4, in order to contribute the improvement of the accurate prediction on the RMP penetration threshold in the Ohmic tokamak discharges, in the LHD plasmas without any external torque, the empirical scaling of the RMP penetration threshold on the electron density and the beta value is shown. Finally, we give a brief summary.

2. EXPERIMENTAL SETUP

The LHD is a heliotron device with a pair of helical coils and three pairs of poloidal coils. The typical major and minor radii are 3.6m and 0.65 m, respectively. The helical coils consist of three layers winding coils built in the minor radial direction. We can change the plasma aspect ratio and the magnetic shear, the magnetic hill parameter due to change the minor radial location of the helical coil current centre, that is, the helical coil pitch parameter, $\gamma_C \equiv (M/l)/(R_C/a_C)$, where M and l are the toroidal field period and the number of poles of the helical coils, and R_C and a_C are the major and the minor radius of the helical coil winding law, respectively. In this paper, the plasma aspect ratio, A_p, changes from 5.7 to 7.1 (γ_C=1.254~1.174). The central rotational transform changes from 0.33 to 0.57, but the edge rotational transform is maintained around 1.65, which suggests that the magnetic shear decreases with the increase of A_p. The magnetic hill parameter increases with the increase of A_p. And the m/n=1/1 resonant rational surface moves from 0.85 to 0.73 as the function of the normalized minor radius [20]. Here m and n are the poloidal and toroidal mode numbers. LHD equips ten pairs of coils with normal conductors set at the top and the bottom (RMP coils), which can produce a magnetic field of m/n = 1/1 and/or 2/1 modes with a different phase. In this study, the perturbation field with m/n=1/1 is imposed by RMP coils.

We carried out ramp-up RMP experiments. The typical discharge time and operational magnetic field is 2s and 1.38T, respectively. Figure 2 shows a typical waveform of the ramp-up RMP experiment with A_p=7.1 configuration. The plasmas are initiated by ECH, and they are maintained by the 2 tangential NBs, which are injected in order to balance the NBI currents and the external torque as shown in Fig.2(a). It is a similar condition with the Ohmic tokamak plasmas. The perpendicular NBs with the positive ion sources are intermittently injected to measure the poloidal and toroidal plasma flow velocities, as shown in Fig.2(b). During

the discharge with almost constant density and heating power as shown Figs.2(a) and (b), the external RMP coil current increases as shown in Fig.2(c). Here it should be noticed that the externally imposed RMP does not rotate, and $I_{RMP\text{-}p}/B_t$=1kA/T corresponds to the magnetic island with the 20% of the minor radius as the size. The RMP current was ramped up with 0.3 kA/s. In Fig.2(d), at t~4.55s, the phase of the RMP induced by plasmas, which is measured by two pairs of saddle coils set located in different toroidal section, suddenly changes and a flat structure around the resonant rational surface suddenly appears in the electron temperature radial profile. In this paper, the RMP coil current ($I_{RMP\text{-}p}$) is identified as an index of the RMP penetration threshold as shown in Fig.2(c). Figure 2(e) shows the time evolution of the poloidal rotation speed around the resonant surface.

In section 3.3, we show the RMP penetration threshold dependence for the various plasma aspect ratio configurations. According to Ref.[7], the magnetic shear and/or the magnetic hill parameter are key parameters of the RMP penetration. They are strongly related to the Mercier index, D_I, which is an index for the ideal interchange instability. Figure 3(a) shows D_I at the ι=1 rational surface with <β>~1%. D_I increases with the increase of A_p. On the other hand, according to Ref.[17], the neoclassical viscous torque would be another key parameter. The neoclassical viscous torque is strongly related with the magnetic field ripple, then the dependence on the plasma aspect ratio is shown in Fig.3(b). Here ε_h, ε_{h+1} and ε_{h-1} are the helical magnetic ripple and its poloidal side band components, ε_t and ε_b are the toroidal and bumpy magnetic ripples, respectively. ε_h and ε_t decrease with the increase of A_p, and the ratio between ε_{h+1} + ε_{h-1} and ε_h increases with the increase of A_p.

3. RMP PENETRATION THRESHOLD DEPENDENCE IN THE LHD

3.1. Plasma aspect ratio dependence of the penetration threshold

In Ref.[7], the penetration threshold dependence on the plasma aspect ratio is investigated under almost the same beta and collisionality regimes in the LHD. There we found that the RMP penetration threshold decreases with the increase of the plasma aspect ratio. Now we investigate the penetration threshold dependence on the collisionality of ion for the various aspect ratio plasmas (A_p=5.7, 6.1 and 7.1). The results are shown in Fig.4. Here ν_{i*b}=1 means the ion collisionality boundary between the plateau and the banana regimes, and A_p=5.7, 6.7 and 7.1 are shown by ○, ▼ and ◇, respectively. Then, the plasmas are in between the plateau and the banana regimes, and in almost the 1/ν-collisional regime because the helical magnetic ripple is almost twice larger than the toroidal one as shown in Fig.3(b), ν_{i*h}~3 ν_{i*b}. Here ν_{i*h}=1 means the ion collisionality boundary between the helical plateau and the 1/ν regimes. It should be noted that β_{local} ~0.35% at A_p=5.7 and β_{local} ~0.48% at A_p=7.1, which corresponds to both the volume averaged beta values are around 1.0% because the resonant magnetic surface of A_p=7.1 is located inner than that of A_p=5.7. These beta regimes are less than those in Ref.[7].

The most impressive result in Fig.4 is that the penetration threshold dependence on the collisionality in the low plasma aspect configuration, A_p=5.7 is opposite in the high aspect one, A_p=7.1. That's, the threshold of A_p=5.7 scales with $\nu_{i*b}^{0.40}$, and that of A_p=7.1 does with $\nu_{i*b}^{-0.10}$. Here the correlation coefficients, R, are 0.67 and 0.97, respectively. Only in a high collisional regime, ν_{i*b}>1 (almost plateau regime), the threshold dependence on the plasma aspect ratio in Ref.[7] is reproduced. In a low collisional regime, ν_{i*b}<1 (almost banana regime), another dependence appears. This result would lead to the reconsideration of the statement that the index of the MHD instability, such as the Mercier parameter should strongly affect the penetration threshold [7] because both the magnetic shear and the magnetic hill parameter change little when the beta value is maintained even though the collisionality changes as shown in Fig.4.

3.2. Ion species dependence of the penetration threshold

Recently, the deuterium experiments started in the LHD [21]. Here, in the deuterium discharges, the ions injected by the balanced NB and the perpendicular NB are deuterium in addition to the working gas supplied by gas-puff systems. We compare the RMP penetration thresholds in the deuterium and the hydrogen discharges with the very similar beta regime. Figure 5 shows the threshold dependence on the collisionality in the hydrogen and the deuterium discharges. The plasma aspect ratio is A_p=5.7, the magnetic axis torus-location is 3.6m and β_{local} ~0.30%, which is lower than those in Fig.4. The penetration threshold in hydrogen plasmas scales with $\nu_{i*b}^{0.40}$, and that in deuterium plasmas does with $\nu_{i*b}^{0.93}$. Here Rs are 0.98 and 0.77, respectively. That,s, the thresholds in both deuterium and the hydrogen increase with the increase of the collisionality as same with ○ in Fig.4. From Fig.5, the penetration threshold in the deuterium discharges is smaller than that in the hydrogen discharges in the same collisionality regime. This result means that the deuterium plasmas are affected with the

smaller external RMP than in the hydrogen, which leads to the unfavourable property because the tolerance of the error field to prevent the degradation due to the appearance of magnetic island in the deuterium discharges is smaller than that in the hydrogen discharges.

3.3. Relationship between RMP penetration threshold and plasma poloidal velocity

Here we consider the reason why the RMP penetration threshold dependence on the collisionality appears for the various magnetic configurations and ion species, as shown in sections 3.1 and 3.2. The most popular model on the shielding mechanism of the external RMP is a balance between the electro-magnetic and the viscous torque [11], which is based on the following scenario. When the plasma is rotating at a relatively large speed, the large difference between two Alfven resonant surfaces due to the large plasma speed prevents the reconnection of the magnetic field lines because the Alfven resonance does not overlap with the resonant surfaces [22]. When the external RMP exists, the plasma rotation is driven by a viscosity torque, at the same time, the rotation is decelerated by the electro-magnetic torque by the externally imposed RMP and its driving perturbed plasma current. Then when the electro-magnetic torque is beyond the viscous torque, the plasma rotation is decelerated and the external RMP penetrate the resonant rational surfaces. According to a model in helical plasmas without an external torque [23], the poloidal neoclassical viscosity is considered dominant, and the effect of an index related with the MHD instability on the penetration threshold is expected to be small. The neoclassical viscous torque is expressed by the product of a poloidal rotation speed and a viscosity coefficient, and the electro-magnetic torque is roughly proportional to the square of the externally imposed RMP coil current. The imposed RMP coil current, when RMP penetrates, corresponds to the index of the penetration threshold, $I_{\mathrm{RMP\text{-}p}}$. On the contrary, the neoclassical poloidal rotation and the viscous coefficient are considered to depend on the ion species and the configuration through the helical ripple in the magnetic field strength and the rotational transform.

Figure 6 shows the poloidal plasma rotation ($\omega_{\mathrm{pol@\iota=1}}$) of the plasma at the rational surface just before the penetration as the function of the collisionality in the deuterium and hydrogen discharges. The dataset is included by that of Fig.5. This figure shows that the poloidal rotation in the deuterium discharges is much smaller than that in the hydrogen discharges when we compare them at the same collisionality, which would lead to the reduction of the penetration threshold in the deuterium discharges. Next, we plot the penetration thresholds of Fig.4 (A_p=7.1;◇, A_p=5.7;○) and Fig.5 (H;●, D;■) as the function of the poloidal rotation as shown in Fig.7. In all cases, the RMP penetration thresholds increase as the poloidal rotation is faster, which is qualitatively consistent with the torque balance model between the electro-magnetic and the poloidal viscous torque [23, 24]. Then the main reason, why the penetration threshold in the deuterium is lower than that in the hydrogen, is considered that the poloidal rotation in the deuterium is slower than that in the hydrogen. The opposite dependence of the penetration threshold on the collisionality in the various plasma aspect configurations would come from the poloidal rotation dependence on the collisionality.

Figure 8 shows the poloidal rotation frequency at the resonant surface as the function of an index of the neoclassical flow in the deuterium and hydrogen plasmas of Fig.6. Because the neoclassical poloidal rotation speed for the same configuration would be approximately proportional to $T_e*(n_e'/n_e+2T_e'/T_e)$ according to Ref.[23], $T_e*(n_e'/n_e+2T_e'/T_e)$ is defined as the index of the neoclassical flow here. Figure 8 shows that the poloidal rotation frequency of deuterium is relatively larger than that of hydrogen around same collisionality. However, both the rotations of deuterium and hydrogen don't have clear dependence on the index of the neoclassical flow. It should be noted that the neoclassical poloidal flow depends on the radial electric field exactly speaking, in Ref.[23], the radial field is expressed by n_e'/n_e and T_e'/T_e with a simple assumption. Moreover, on the neoclassical poloidal flow velocity in the various plasma aspect configurations, it depends on the magnetic configuration in addition to the above index of the neoclassical flow. That is, the neoclassical poloidal viscosity is proportional to the non-axisymmetric neoclassical radial particle flux [25], which has different dependence on the collisionality and the magnetic field ripple component [26, 27]. The comparison between the neoclassical prediction taking the radial electric field, the collisionality and the magnetic field into account, and the observed poloidal rotation is a future subject.

4. COMPARISON BETWEEN BALANCED NBI HELICAL PLASMAS AND OHMIC TOKAMAK PLASMAS

As shown in section 1, in Ohmic discharges of tokamaks, the tokamak researchers are constructing the following RMP penetration threshold scaling [28], and checking the validation through the multi-device experiments for the various density (n_e) and beta (β_N) regimes from the viewpoint of the avoidance of the locked mode instability in ITER operation.

$$B_{pen}/B_t \propto n_e^{1.4\pm0.13} B_t^{-1.8\pm0.16} R^{0.81\pm0.24} \beta_N^{-0.86\pm0.14}$$

Here B_{pen} denotes the amplitude of the RMP penetration threshold, and B_t and R are the toroidal magnetic field strength and the major radius, respectively. We investigate the RMP penetration threshold dependence on the density and the beta value in the LHD with A_p=5.7 for the m/n=1/1 mode. The A_p=5.7 configuration corresponds to a high confinement performance configuration in the LHD experiments. Figure 9 shows the penetration threshold as the function of the density at the resonant rational surface. Here the plasmas are heated by the balanced tangential NBIs, which corresponds to the similar condition of tokamak's Ohmic discharges in the sense that there is no external torque. The collisionality belongs to the plateau regime. The penetration thresholds for the cases that the beta value at the m/n=1/1 resonant rational surface (β_{local}) is around 0.35% and 0.30%, and are shown by ○ and ●, respectively. The penetration threshold of β_{local}~0.35% and ~0.30% scales with $n_e^{0.87}$. Here Rs are 0.94 and 0.99, respectively. That's, the power laws of the thresholds on the electron density are similarly independent of beta regimes, which is qualitatively similar with that of tokamaks, but it has quantitatively weak dependence ($\propto n_e^{0.87}$) on the density with tokamaks ($\propto n_e^{1.4}$). On the other hand, the threshold in the LHD is larger as the beta increases, which is different from tokamaks.

5. SUMMARY

We investigate the penetration threshold of the RMP by the external coils in the LHD for the various plasma aspect ratio configurations. According to the RMP ramp-up experiments with the almost 1/ν-collisional regimes under the balanced-NB heating, the qualitative dependence on the collisionality in a low plasma aspect configuration is opposite to that in a high plasma aspect one, which is a quite unique property compared with the tokamaks, and is first found in the LHD. We also investigate the threshold dependence on the ion species, and find that the threshold of deuterium is quite smaller than that of hydrogen. Figure 10 shows the operational regimes of RMP penetration threshold experiments, as shown in Figs.2 and 3, in the electron density and the collisionality diagram, n_e and ν_{i*b}. Here, A_p=5.7~7.1 and β_{local} =0.3, 0.35 and 0.48%. In all the above cases, the RMP penetration thresholds are higher as the poloidal rotation is faster, which shows that the poloidal rotation is the dominant driver to the RMP threshold and this effect is borne out in both ion mass and aspect ratio studies. The fact is qualitatively consistent with the torque balance model between the electro-magnetic and the poloidal viscous torque. Moreover, we compare the relationship between the poloidal flow velocity and the flow index predicted by a neoclassical theoretical model. However, the observed flow velocity is not consistent with the neoclassical prediction with a simple assumption taking the radial electric field effect into account. The evaluation of the neoclassical flow velocity consistently including the radial electric field and the comparison between that and the observation is one of future subjects.

In a good confinement configuration (A_p=5.7) of the LHD without external toroidal and poloidal torque input like an unbalanced NBI, the threshold dependence on the density is qualitatively similar with that in Ohmic tokamak plasmas, but the beta dependence is opposite to the tokamaks. In Ohmic tokamak plasmas, the anomalous viscous torque is expected to be much more dominant compared with the neoclassical viscous torque [23, 24]. However, the prediction of the RMP penetration condition in helical plasmas with the high accuracy would lead to the systematic understanding of the penetration mechanism in torus plasmas because in the higher collisionality region in the LHD there is a possibility that the anomalous viscosity is dominant instead of the neoclassical viscosity as the viscous torque.

ACKNOWLEDGMENTS

This work was supported in part by JSPS KAKENHI (No.25289342) and by NIFS under contracts ULPP022 and NIFS07KLPH004, by a Grant-in-Aid of Future Energy Research Association. The authors are grateful to the LHD operation group for their excellent technical support. One of the authors (K.Y.W) thanks Professors S. Nishimura and M. Furukawa for their fruitful discussion.

REFERENCES

[1] M. OKABAYASHI et al., Plasma Phys. Control. Fusion 44 (2002) B339.
[2] T.E. Evans et al., Phys. Plasmas 13 (2006) 056121.
[3] Y. TAKEIRI et al., Nucl. Fusion 57 (2017) 102023.
[4] N. OHYABU et al., Phys. Rev. Lett. 88 (2002) 055005.

[5] Y. NARUSHIMA et al., Nucl. Fusion 48 (2008) 075010.
[6] N. OHYABU et al., Plasma Phys. Control. Fusion 47 (2005) 1431.
[7] S. SAKAKIBARA et al., Nucl. Fusion 53 (2013) 043010.
[8] R. BUTTERY et al., Nucl. Fusion 39 (1999) 1827.
[9] Y. KIKUCHI et al., Phys. Rev. Lett. 97 (2006) 085003.
[10] R. BUTTERY et al., Nucl. Fusion 51 (2011) 073016.
[11] R. FITZPATRICK, Nucl. Fusion 39 (1993) 1049.
[12] J.-K. PARK et al., Nucl. Fusion 51 (2011) 023003.
[13] M. KOBAYASHI et al., Nucl. Fusion 53 (2013) 093032.
[14] K. TOI et al., Nucl. Fusion 54 (2014) 033001.
[15] H. YAMADA et al., Contrib. Plasma Phys. 50 (2010) 480.
[16] Y. NARUSHIMA et al. Nucl. Fusion 51 (2011) 083030.
[17] Y. NARUSHIMA et al. Nucl. Fusion 55 (2015) 073004.
[18] Y. NARUSHIMA et al. Nucl. Fusion 57 (2017) 076024.
[19] K. NARIHARA et al., Phys. Rev. Lett. 87 (2001) 135002.
[20] K.Y. WATANABE et al., Fusion Sci. Technol. 58 (2010) 160.
[21] M. OSAKABE et al 2017 Fusion Sci. Technol. 72 199
[22] A. BOOZER et al., Phys. Plasmas 10 (2003) 1458.
[23] S. NISHIMURA et al., Phys. Plasmas 19 (2012) 122510.
[24] C. C. HEGNA, Phys. Plasmas, 19 (2012) 056101.
[25] K. C. SHAING and J. D. CALLEN, Phys. Fluids 26 (1983) 3315.
[26] K. C. SHAING, Phys. Fluids 27, (1984) 1567.
[27] K. C. SHAING et al., Phys. Fluids 29 (1986) 521.
[28] Y. GIRBOV, in Meeting of ITPA MHD TG, Oct. 2017 (Barcelona, Spain).

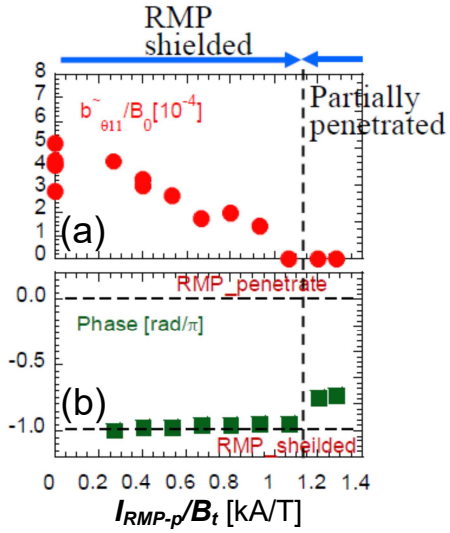

FIG. 1. The magnetic fluctuation amplitude (a) and the phase (defined by the poloidal location of the island's O-point at a toroidal cross-section) of m/n=1/1 RMP component induced by plasma as the function of the imposed RMP coil current. The vertical dashed line denotes the boundary between the RMP is shielded and theRMP partially penetrates.

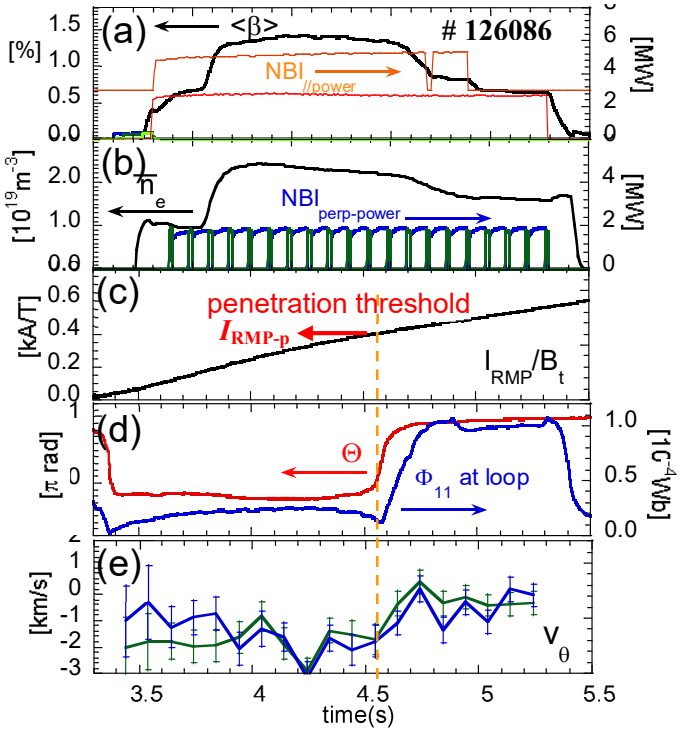

FIG.2. Typical discharge waveform for RMP ramp-up experiment. (a) the volume averaged beta and tangential NBI port-through-power for 2 beam lines, (b) the line averaged electron density and perpendicular NBI port through power, (c) the external RMP coil current, (d) The phase (defined by the poloidal location of the island's O-point at a toroidal cross-section) and amplitude m/n=1/1 RMP component induced by plasma, Θ and Φ, (e) the poloidal flow velocity around the resonant rational surface. The vertical dashed line corresponds to the time when the external RMP penetrates

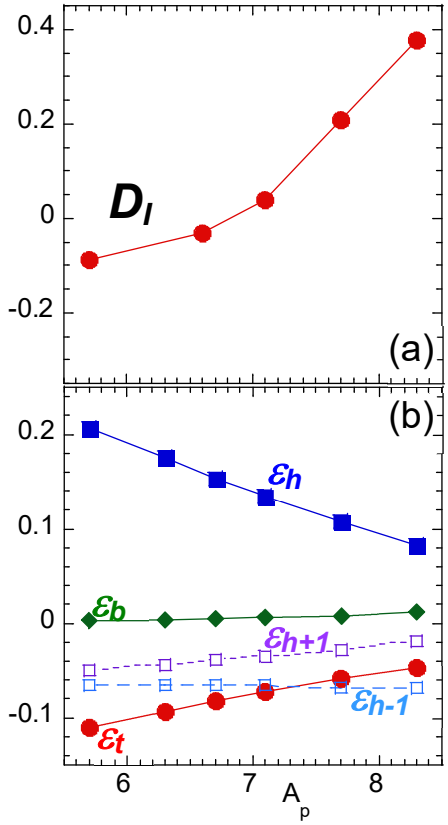

FIG. 3.(a) D_I at the iota=1 rational surface with <β>~1% and (b) Magnetic field ripple components as the function of A_p. Here ε_h, ε_{h+1}, ε_{h-1} are the helical magnetic ripple and its poloidal side band components, ε_t and ε_b are the toroidal and bumpy magnetic ripples, respectively.

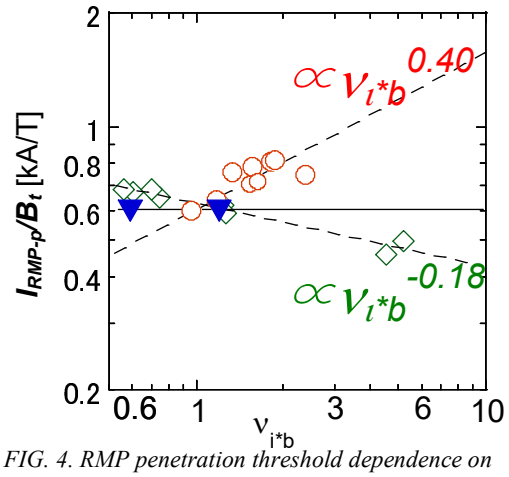

FIG. 4. RMP penetration threshold dependence on collisionality for various A_p configurations in the LHD. ν_{i*b}=1 means the boundary of the plateau and the banana regimes. A_p=5.7, 6.7 and 7.1 are shown by ○, ▼ and ◇, respectively.

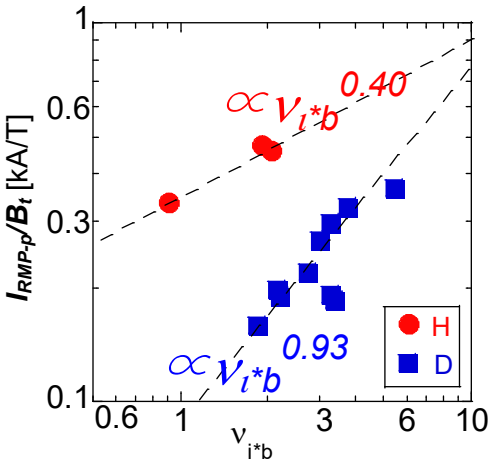

FIG. 5. RMP penetration threshold as the function of the collisionality in the LHD with A_p=5.7 and β_{local}~0.3%. Here the deuterium and hydrogen discharges are shown by ■ and ●, respectively.

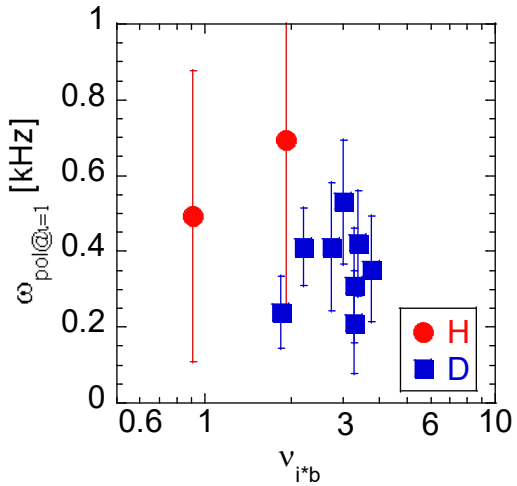

FIG.6. Poloidal rotation frequency at the m/n=1/1 resonant rational surface as the function of the collisionality. Here the deuterium and hydrogen discharges are shown by ■ and ●, respectively.

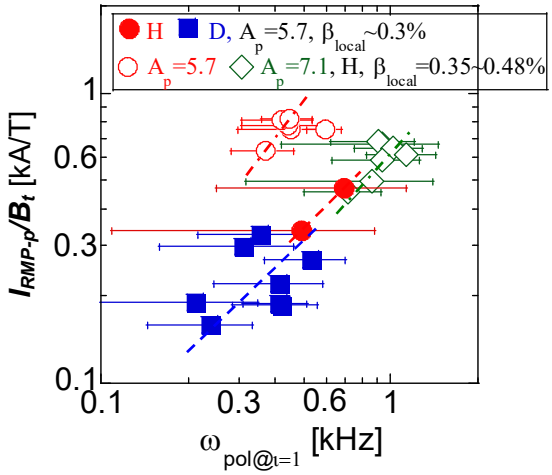

FIG.7. RMP penetration threshold as the function of $\omega_{pol@t=1}$ in the LHD with A_p=5.7~7.1 and β_{local} =0.3, 0.35 and 0.48% as shown in Figs.2 and 3. Dashed, and a dash and dot lines denote the auxiliary lines to show a trend.

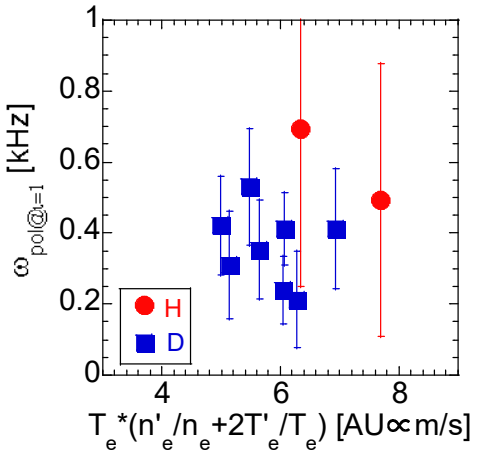

FIG. 8. Poloidal rotation frequency at the m/n=1/1 resonant rational surface as the function of an index of the neoclassical flow. Here the deuterium and hydrogen discharges are shown by ■ and ●, respectively.

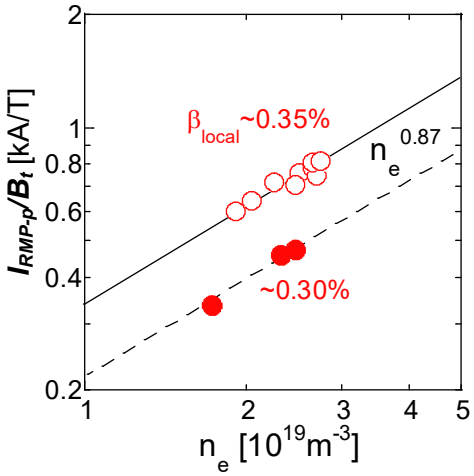

FIG. 9. RMP penetration threshold as the function of the density at the rational surface in the LHD with A_p=5.7 for the m/n=1/1 mode. Here β_{local} ~0.35% (○) and ~0.30% (●) are shown.

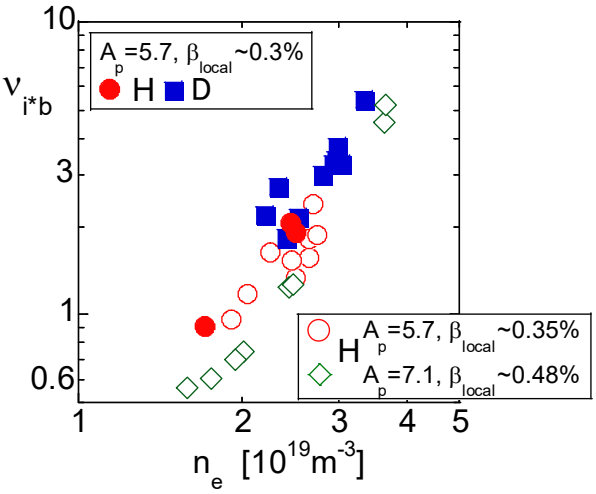

FIG. 10. Operational regimes of RMP penetration threshold experiments in the electron density and the collisionality diagram, n_e and ν_{i*b}. A_p=5.7~7.1 and β_{local} =0.3, 0.35 and 0.48% as shown in Figs.2 and 3.